CHEMISTRY
A EUROPEAN JOURNAL

Solution Conformation and Dynamics of the Ion Pairs Originating from the Reaction of $B(C_6F_5)_3$ with Bisindenyl Dimethyl Zirconium Complexes

Tiziana Beringhelli,[a] Giuseppe D'Alfonso,*[a] Daniela Maggioni,[a] Pierluigi Mercandelli,*[b] and Angelo Sironi[b]

Abstract: The two ion pairs $[(4,7\text{-}Me_2indenyl)_2ZrMe]^+[MeB(C_6F_5)_3]^-$ (**1b**) and $[(indenyl)_2ZrMe]^+[MeB(C_6F_5)_3]^-$ (**2b**) have been generated in situ by reaction of stoichiometric $B(C_6F_5)_3$ with the corresponding dimethyl zirconocenes. It has been shown that molecular mechanics computations, guided by experimental $^1H/^1H$ NOE correlations, can provide information on the conformers present in solution. The dynamics of the ion pairs has also been investigated, showing the occurrence of both the processes previously characterized for this class of compounds, namely the $B(C_6F_5)_3$ migration between the two methyl groups and dissociation–recombination of the whole $[MeB(C_6F_5)_3]^-$ anion, the latter process being much faster than the first one (about three order of magnitude). Moreover, it has been shown that in certain conditions intermolecular processes can occur, which mimic the above-mentioned dissociative exchanges. In particular, the presence of species containing loosely bound $[MeB(C_6F_5)_3]^-$ anion fastens the exchange of this anion, while the presence of free $B(C_6F_5)_3$ accelerates its exchange between the two methyl sites.

Keywords: boranes · ion pairs · metallocenes · molecular modeling · NMR spectroscopy

Introduction

Many Lewis acids containing Group 13 elements have been successfully used in the last decade as activators of the metallocene single-site catalysts for olefin polymerization.[1] These acids act as cocatalysts, by removing an R^- group from the catalyst precursor (the metallocene) to give an ion pair constituted by the coordinatively unsaturated cation and the anionic adduct between the acid A and the R^- group [Eq. (1)]. The stability and the dynamics of these ion pairs greatly influence the effectiveness of the catalyst and the characteristics of the polymerization process.[1]

$$Cp_2MR_2 + A \rightleftharpoons [Cp_2MR]^+ \cdots [RA]^- \quad (1)$$

Fluoroarylboranes, and in particular the progenitor tris(pentafluorophenylborane) $B(C_6F_5)_3$,[2] are among the more commonly used and effective activators. They give contact ion pairs, that have been isolated and even X-ray characterized in the solid state,[3–6] showing that the anion occupies the vacant coordination site of the metal (inner-sphere ion pair), with the B-bound R group (actually a methyl) in bridging position between B and Zr (its distance from the Zr atom being significantly longer than that of the true methyl ligand).

Even if the ion pair is relatively tight, thorough studies[3,6–8] established the occurrence in solution of two types of dynamic processes involving the borane moiety, shown in Scheme 1 for the prototypical zirconocenium/$B(C_6F_5)_3$ catalyst $[(1,2\text{-}Me_2Cp)ZrMe]^+[MeBAr(C_6F_5)_2]^-$.[7] Both the processes lead to dynamic symmetrization of the ion pair by the exchange of the anion from one side of the zirconocene to the other (without cleavage of the Me–B bond) or by the exchange of the borane between the two Me–Zr groups. The two processes can be distinguished through ^1H NMR

[a] Prof. T. Beringhelli, Prof. G. D'Alfonso, Dr. D. Maggioni
Università di Milano, Facoltà di Farmacia
Dipartimento di Chimica Inorganica, Metallorganica e Analitica
via Venezian 21, 20133 Milano (Italy)
E-mail: giuseppe.dalfonso@istm.cnr.it

[b] Dr. P. Mercandelli, Prof. A. Sironi
Università di Milano, Dipartimento di Chimica Strutturale
e Stereochimica Inorganica and CNR
Istituto di Scienze e Tecnologie Molecolari
via Venezian 21, 20133 Milano (Italy)
E-mail: pierluigi.mercandelli@unimi.it

Supporting information for this article is available on the WWW under http://www.chemeurj.org/ or from the author: Figure showing details of the NMR data, plots of the kinetic constants, and force field description and validation.

DOI: 10.1002/chem.200400609

analysis, since the second one causes dynamic equalization not only of the diastereotopic protons within the π ligands (as the first one), but also of the two Me groups bonded to the metal atom.

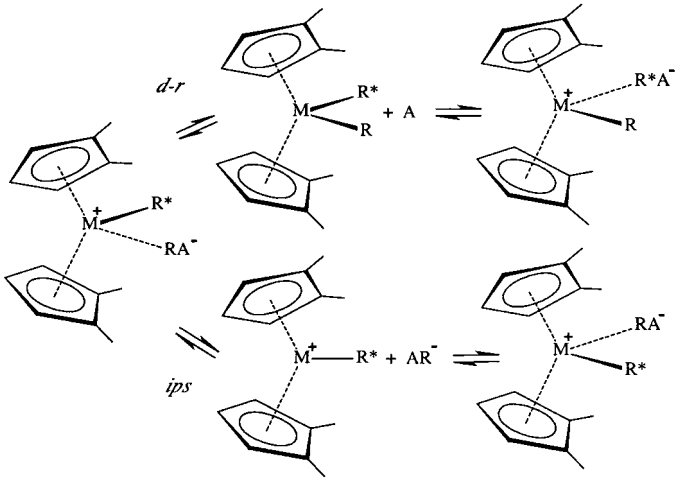

Scheme 1. Two dynamic processes leading to symmetrization of the Cp-like ligands: ion-pair separation (*ips*) or borane dissociation–recombination (*d–r*).

The abbreviation *ips* (ion-pair separation) has been proposed for the first process and *d–r* (dissociation–recombination) for the second one,[7] since dissociative mechanisms were suggested for both the processes by the experimental results concerning a series of $[(1,2\text{-}Me_2Cp)MMe]^+[MeBAr(C_6F_5)_2]^-$ ion pairs, containing different Ar substituents on boron and M = Zr or Hf.

By contrast, a successive study of the anion exchange kinetics in $[L_2ZrMe]^+[MeB(C_6F_5)_3]^-$ ion pairs, generated in situ by reaction of $B(C_6F_5)_3$ with various *ansa*-zirconocene dimethyl complexes, suggested that anion exchange occurred by way of ionic aggregates (such as ion quadruples), rather than via dissociation of solvent-separated ions.[6] However, a very recent study, employing both cryoscopy and pulsed field gradient spin-echo NMR diffusion measurements, did not provide evidence of significant aggregation for ion pairs containing the methyl borate anion in the inner sphere (whilst a tendency to form higher aggregates was found for metallocenium cations with outer sphere anions).[9]

We have now investigated the dynamics in $[D_8]$toluene of the ion pairs formed in situ by interaction of $B(C_6F_5)_3$ with the bisindenyl dimethyl zirconium complexes of Figure 2 and we have got evidence that in particular conditions (presence of free borane or of "free" methylborate anion or of adventitious impurities) intermolecular processes can occur, that contribute to indenyl symmetrization and emulate the *d–r* or *ips* processes.

Moreover we have shown that, in spite of the high mobility of these systems, information on their solution structures can be obtained by combining NOE data and computational

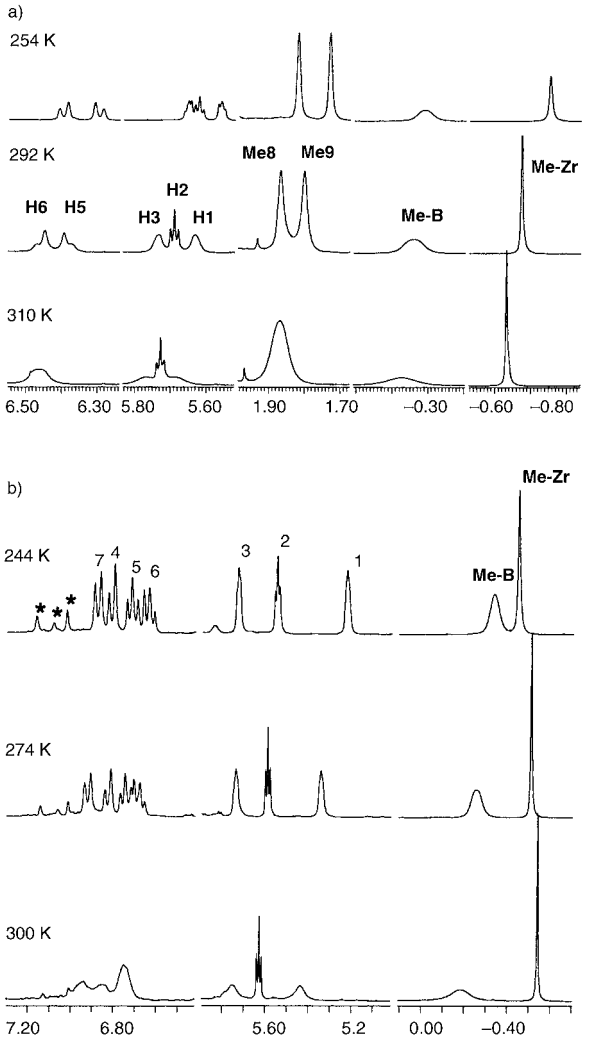

Figure 1. Variable temperature ^1H NMR of a) **1b** (32 mM) and b) **2b** (46 mM); the asterisks mark the signals of the solvent (the intensities of these signals increase at low temperature due to faster relaxation).

analysis. These studies not only confirmed that such species exist in solution as inner-sphere ion pairs, but also provided a picture of the preferred rotational isomers present in solution.

Results and Discussion

Solution structures of $[(4,7\text{-}Me_2indenyl)_2ZrMe]^+[MeB(C_6F_5)_3]^-$ (1b) and $[(indenyl)_2ZrMe]^+[MeB(C_6F_5)_3]^-$ (2b): The two zirconocene complexes $[(4,7\text{-}Me_2indenyl)_2ZrMe_2]$ (**1a**) and $[(indenyl)_2ZrMe_2]$ (**2a**)[10] exhibit in solution an apparent C_{2v} symmetry, higher than the C_2 symmetry observed in the solid-state structure of **2a**.[11] This indicates rapid rotation of the two indenyl ligands around the Zr–indenyl vector, causing the dynamic averaging of different conformations, in line with the very low torsional energy barrier of $[(indenyl)_2MX_2]$ bent metallocenes.[12]

The addition of one equivalent of $B(C_6F_5)_3$ to toluene solutions of **1a** or **2a** causes the instantaneous formation of adducts **1b** or **2b**. Their ^1H (Figure 1) and ^{13}C NMR spectra still show the equivalence of the two indenyl moieties (apparent C_s symmetry even at 190 K),[17] indicating that even in the ion pairs the two indenyl rings enjoy a conformational freedom sufficient to create a pseudo mirror plane.

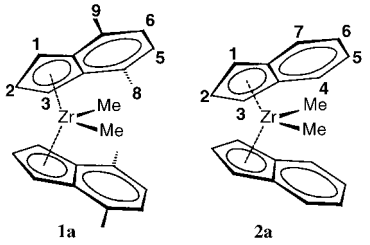

Figure 2.

The indenyl protonic resonances have been assigned through their low temperature mutual dipolar correlations (**1b**, Figure 3) and through their scalar correlations (**2b**, Figure S1 of Supporting Information). In both the adducts, the two high-field signals of the Zr-bound and B-bound methyl groups (hereafter Me–Zr, and Me–B, respectively) were straightforwardly assigned, due to the broadening of the latter signal for the coupling with the quadrupolar boron isotopes.

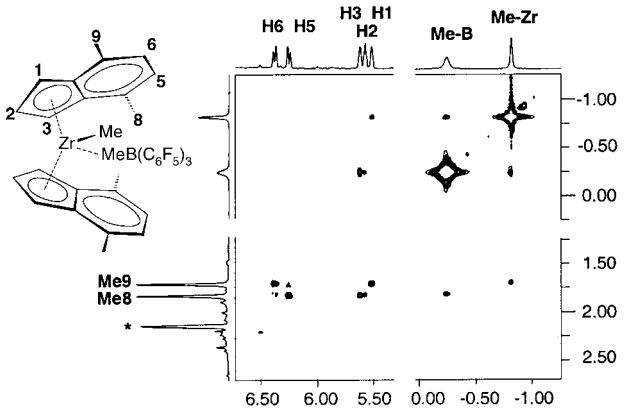

Figure 3. Selected regions of a ^1H NOESY experiment on **1b** (211 K, RD = 3 s, τ_m = 0.2 s, 12.5 mM). The asterisk marks a toluene resonance.

The NOESY experiments also provided information about the torsional isomers present in solution, based on the correlations between the indenyl protons and the Me–Zr and Me–B groups. In particular, in **1b** (Figure 3) Me–Zr exhibits NOE correlations with the methyl group in position 7 (Me9) and with H1, whilst Me–B correlates with the methyl in position 4 (Me8) and with H3. Such correlations imply that the two indenyl rings do not enjoy complete rotational freedom around the Zr–indenyl axis (since this would provide correlations of the same intensity with the protons on both the ring sides), but rather oscillate between limit conformations. Moreover, the presence of specific H1/H3 (not shown) and H2/Me8 dipolar cross peaks (Figure 3) lays down some constraints on the mutual orientation of the π ligands, since these correlations can arise from *inter*-ring interactions only.

In the case of the ion pair **2b**, the NOE data (Figure 4 and S2, Supporting Information) suggest again the presence of one or more preferred rotamers: Me–Zr correlates mainly with H2 and H3, and, to a minor extent, with H4 (and H1) while Me–B has correlations with H3, H4, and H1. As far as inter-ring interactions are concerned, dipolar cross-peaks are observed between H1/H3 and H2/H7 (Figure S2).[18]

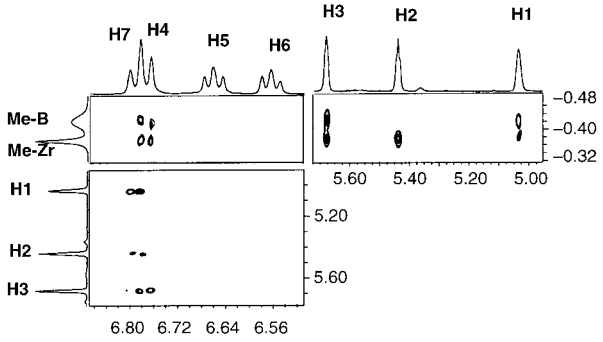

Figure 4. Selected regions of a ^1H NOESY experiment on **2b** (11 T, 215 K, RD = 3 s, τ_m = 0.25 s, 29 mM).

In order to extract conformational information from the observed pattern of NOE intensities a molecular mechanics study has been undertaken, employing a force field parameterized on purpose to describe the geometry of the ion pair (see Experimental Section).[19]

Structural analysis of small to medium-sized species are usually faced by a preliminary search of the low energy isomers (or conformations) of the molecule and by a subsequent check of their agreement with the observed NOE pattern.[19] In the case of large-sized molecules, NOE intensities are instead turned into a set of restraints to be used in distance geometry or molecular dynamics calculations.

Due to the paucity of experimental energy data available for this class of compounds, our force field has been parameterized to reproduce geometries only and a *direct* search of the more stable rotamers for the two complexes is not viable. Moreover, for our system an important dependence of the molecular conformation on the solvent can be anticipated and the comparison of the outcomes of a conformational analysis in vacuo with experimental data in solution can be questionable. At the same time, distance geometry or restrained molecular dynamics are difficult to apply to our system since, due to the dynamic processes that lead to an apparent C_s symmetry of the ion pairs and to the possible presence of more than one rotamer in fast interconversion, the observed intensities cannot be *directly* changed into a suitable set of interproton distances.[19]

However, assuming the $B(C_6F_5)_3$ moiety adopts the usual chiral disposition of the three aryl substituents, conformations of **1b** and **2b** can be completely described by just two torsional angles involving the Zr–cp axes, namely cp′-Zr-cp-C2 (τ_1) and cp-Zr-cp′-C2′ (τ_2) (cp refers to the centroid of the indenyl five-membered ring; normal and primed atoms refer to the "upper" and "lower" rings as depicted in Figures 5 and 6).

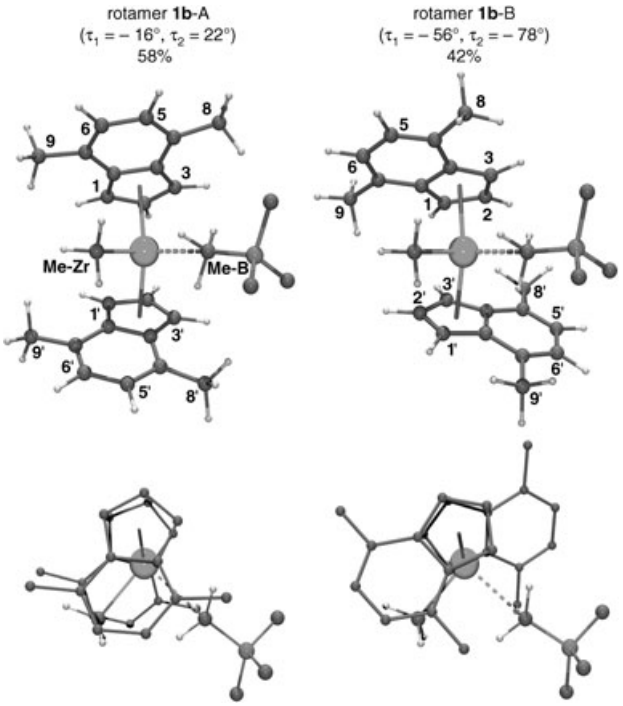

Figure 5. Front and top views of the two proposed rotamers for the ion pair **1b**. For clarity, hydrogen atoms of the indenyl moieties have been omitted in the top view.

We decided to tackle the conformational problem by optimizing a large set of possible structures for each ion pair, constraining the τ_1 and τ_2 torsional angles at fixed values from −180 to +180° in steps of 18°. For each generated structure a set of effective distances $d_{ij,effective}$ has been computed taking into account the two processes implied in the averaging of the interproton vectors, namely the fast rotation of the methyl groups and the enantiomerization process that lead to a dynamic C_s symmetry (see Experimental Section for averaging details).[20]

The effective distances $d_{ij,effective}$ obtained by NOE have been subsequently employed to interpolate the experimental intensities I_{ij}. Due to the expected rotational freedom of the systems under study, we decided to verify the hypothesis that more than one rotamer are contributing to the determination of the observed NOE pattern according to the relationship

$$I_{ij} \propto n_i n_j \sum_{\lambda=1}^{k} w_\lambda (d_{ij,effective})_\lambda^{-6}$$

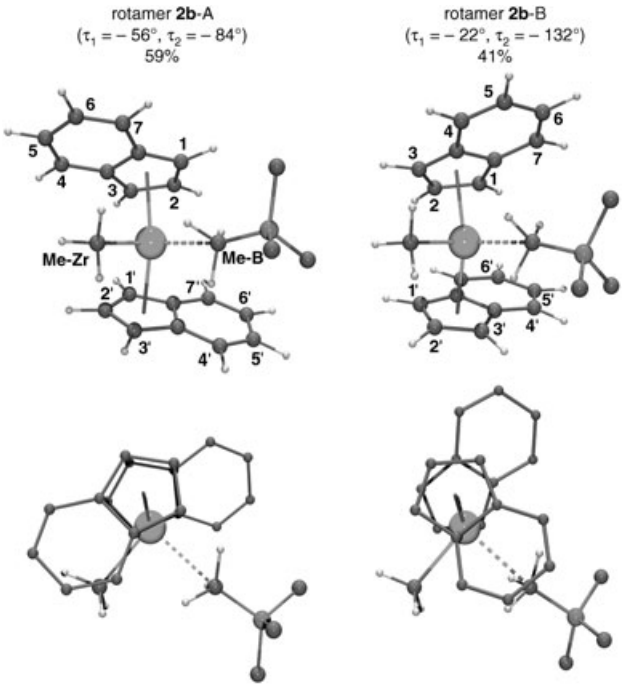

Figure 6. Front and top views of the two proposed rotamers for the ion pair **2b**. For clarity, hydrogen atoms of the indenyl moieties have been omitted in the top view.

in which n_i and n_j are the multiplicities of signals i and j, respectively, w_λ is the relative weight of conformation λ, and k is the number of conformations considered.[21]

The usual determination coefficient r can not be used to assess the effectiveness of adding more conformations to the interpolation process because it always increases as the number of independent parameters in the model increases. Instead, two different criteria can be employed: the increase in the *adjusted* determination coefficient r_{adj},[22] and the significance of the contribution of the different rotamers.[23] For both ion pairs **1b** and **2b**, we found the best description requires two rotamers only: indeed, adding a third one, its contribution resulted to be statistically negligible, and the correspondent value of r_{adj} lowered.

In order to better describe the conformation of the rotamers, a subsequent interpolation has been done employing a finer grid in the vicinity of the previously found optimal structures.[24]

Figures 5 and 6 depict the rotamers proposed for **1b** and **2b**, respectively; while a complete list of averaged interproton distances $d_{ij,effective}$ along with the observed NOE intensities I_{ij} are reported in Tables 1 and 2.

The two rotamers proposed for **1b** (hereafter **1b**-A and **1b**-B) correspond to the ($\tau_1 = -16$, $\tau_2 = 22°$) and ($\tau_1 = -56$, $\tau_2 = -78°$) conformations, respectively. They are present in a ratio of 0.58(7) to 0.42(6), leading to a r_{adj} of 0.925. Rotamer A accounts for the majority of the Me–Zr and Me–B interactions while rotamers B mainly explains the inter-ring crosspeaks and contributes to the Me–Zr/H1 and Me–B/H3 correlations.

Table 1. Experimental NOE intensities I_{ij} for the ion pair **1b** and interproton distances [Å] for the two proposed rotamers.[a]

	I_{ij}[b]	Rotamer **1b**-A		Rotamer **1b**-B	
		I	II	I	II
Me-Zr···H1	0.26	4.14	4.38	5.15	*3.07*
Me-Zr···H2	0.07	5.65	5.73	5.88	3.48
Me-Zr···H3	[c]	5.70	5.56	5.01	5.22
Me-Zr···Me8	[c]	6.18	5.78	4.57	7.42
Me-Zr···H5	0.04	4.90	4.58	3.99	7.72
Me-Zr···H6	0.14	4.05	3.98	4.05	7.10
Me-Zr···Me9	0.88	*3.73*	*3.85*	4.64	5.23
Me-B···H1	0.16	5.49	5.54	5.40	4.03
Me-B···H2	0.24	4.98	4.89	4.08	5.31
Me-B···H3	0.82	*3.38*	*3.42*	*3.00*	5.36
Me-B···Me8	0.98	*3.91*	*3.88*	4.40	5.73
Me-B···H5	[c]	4.77	5.00	5.84	5.06
Me-B···H6	[c]	5.55	5.93	6.71	4.46
Me-B···Me9	0.13	6.35	6.58	6.95	3.99
H1···H3′	1.00	5.73	5.47	*2.34*	6.42
H1···Me8′	0.06	7.95	7.90	3.85	7.40
H1···H5′	[c]	7.84	8.08	6.30	7.18
H1···H6′	[c]	6.88	7.26	7.45	6.73
H2···Me8′	0.29	7.22	6.92	*3.13*	7.52
H2···H5′	[c]	8.17	8.13	4.69	6.62
H2···H6′	[c]	7.93	8.11	6.10	5.37
H2···Me9′	[c]	6.36	6.83	7.21	3.52
H3···H5′	[c]	8.18	7.95	6.04	7.52
H3···H6′	[c]	8.54	8.41	6.65	6.47
H3···Me9′	[c]	7.81	7.93	7.14	4.10
Me8···H6′	[d]	9.70	9.28	8.90	8.88
Me8···Me9′	[c]	9.49	9.25	8.42	6.88
H5···Me9′	[d]	8.73	8.35	9.19	8.97

[a] Short interproton distances are in italics. I and II indicate atoms (I) and primed atoms (II) as shown in Figure 5. [b] Obtained from volume integration of the 2D NOESY cross peaks. [c] Not detectable in the present conditions. For interpolation purpose the I_{ij} value has been set equal zero. [d] In the experimental conditions only *J* cross peaks are observed.[54]

Table 2. Experimental NOE intensities I_{ij} for the ion pair **2b** and interproton distances for the two proposed rotamers.[a]

	I_{ij}	Rotamer **2b**-A		Rotamer **2b**-B	
		I	II	I	II
Me-Zr···H1	0.25	5.04	5.08	5.84	*3.77*
Me-Zr···H2	0.74	5.88	*3.36*	4.75	*3.00*
Me-Zr···H3	0.70	5.10	*3.10*	*3.17*	4.40
Me-Zr···H4	0.48	3.96	5.33	*3.34*	6.51
Me-Zr···H5	[b]	4.03	7.23	5.21	7.89
Me-Zr···H6	[b]	3.98	7.79	6.44	7.72
Me-Zr···H7	[b]	3.91	6.78	6.34	6.07
Me-B···H1	0.38	*3.09*	5.39	4.46	5.39
Me-B···H2	[b]	4.09	5.20	5.47	4.23
Me-B···H3	0.67	5.37	3.81	5.05	*2.89*
Me-B···H4	0.46	6.20	*3.21*	4.29	4.06
Me-B···H5	[b]	6.63	4.45	4.38	5.67
Me-B···H6	[b]	5.74	5.13	4.22	6.58
Me-B···H7	[b]	4.06	5.10	3.66	6.21
H1···H3′	1.00	6.33	*2.38*	5.64	4.01
H1···H4′	[b]	6.21	4.20	4.47	6.36
H1···H5′	[b]	6.33	6.39	3.82	8.14
H1···H6′	[b]	5.83	7.48	3.24	8.42
H2···H4′	[b]	6.05	4.02	5.96	6.40
H2···H5′	[b]	5.73	5.50	5.66	7.85
H2···H6′	[b]	4.33	6.68	4.20	8.26
H2···H7′	0.49	*2.96*	6.69	2.58	7.37
H3···H5′	[b]	7.25	6.93	7.62	7.61
H3···H6′	[b]	6.02	7.25	6.70	7.30
H3···H7′	[b]	3.83	6.75	5.03	6.26
H4···H6′	[b]	8.55	8.87	8.51	6.85
H4···H7′	[b]	6.53	7.56	7.40	5.11
H5···H7′	[b]	8.52	8.46	8.75	5.13

[a] Short interproton distances are in italics. I and II indicate atoms (I) and primed atoms (II) as shown in Figure 6. [b] Not detectable in the present conditions. For interpolation purpose the I_{ij} value has been set equal zero.

The two rotamers for **2b** (hereafter **2b**-A and **2b**-B) correspond to the ($\tau_1 = -56$, $\tau_2 = -84°$) and ($\tau_1 = 22$, $\tau_2 = -132°$) conformations, respectively. They are present in a ratio of 0.59(6) to 0.41(6), leading to a r_{adj} of 0.939. The major rotamer A accounts for both the majority of the Me–Zr and Me–B interactions and the inter-ring cross peaks, while rotamer B mainly accounts for the Me-Zr/H4 and Me-B/H3 correlations.

A survey of the Cambridge Structural Database[25] shows that the different conformations found for **1b** and **2b** are indeed quite common among (indenyl)$_2$MX$_2$ substituted derivatives. The almost C_s symmetric structure of **1b**-A, in which both the indenyl rings are directed toward the front of the molecule, has been found in a variety of *meso ansa*-bridged metallocenes, in particular in [1,1′-C_2H_4(4,7-Me_2indenyl)$_2$]ZrMe_2.[10] The conformation of the almost identical rotamers **1b**-B and **2b**-A,[26] in which an open arrangement of the indenyl moieties embraces the methyl borate anion, has been found instead amongst a great number of racemic *ansa*-bridged metallocene derivatives.

The markedly asymmetric structure of rotamer **2b**-B, in which one of the indenyl ligands eclipses the Zr-Me-B interaction while the other points toward the back of the molecule, might appear unusual. However, it has been previously reported for some unbridged (or bridged by long chains) indenyl derivatives[27] and, more interestingly, for the ion pair [(1,2-Me_2Cp)$_2$ZrMe]$^+$[MeB(C_6F_5)$_3$]$^-$, which can be straightly related to **1b** assuming the two methyl groups substitute for the benzo-condensed ring.[3b]

Dynamic behavior in solution of 1b and 2b: two main conformational processes are operative within ion pairs **1b** and **2b**: The above-discussed oscillation of the two indenyl groups in the cationic moiety, and the fast rotation of the C_6F_5 rings within the [MeB(C_6F_5)$_3$]$^-$ anion.[28] Neither of these motions could be frozen, even at the lowest attainable temperature.

On increasing the temperature, both the ^{1}H (Figure 1) and ^{13}C NMR (for **1b** see Figure S5b of Supporting Information) variable temperature spectra provided evidence of the onset of other dynamic processes.

For **1b**, at first ($T \geq 254$ K) a fluxional process that exchanges all the couples of signals of the indenyl ligand (H1/H3, Me8/Me9, H5/H6, C1/C3, C8/C9, C4/C7, C5/C6, and C3a/C7a) was detected, both by 2D ^{1}H EXSY experiments at 254 and 274 K and band-shape analysis. This is attributa-

ble to the exchange of the anion position (*ips* in Scheme 1), since the resonance of the Me–Zr group did not show any broadening on increasing the temperature up to 300 K. Moreover at 274 K the EXSY map still showed NOE (and not exchange) cross peak between the Me–B and Me–Zr groups.[29]

Only at temperatures higher than 300 K evidence of the occurrence of the *d–r* process (exchange of the borane position, Scheme 1) was obtained. The rate of the latter process ($k \approx 0.02\ s^{-1}$ at 300 K) was much smaller (about three orders of magnitude) than that of anion exchange at the same temperature, in agreement with previous results obtained on other $B(C_6F_5)_3$–metallocene adducts.[30] Indeed the strong Lewis acidity of $B(C_6F_5)_3$ strengthens the Me–$B(C_6F_5)_3$ bond and weakens the $Zr^+\cdots[MeB(C_6F_5)_3]^-$ interaction, with respect to what observed with other weaker Lewis acids.[30]

The behavior of **2b** was completely analogous (see Experimental Section).

Kinetic constants for the exchange processes in the adducts **1b** and **2b** have been evaluated at different temperatures (*ips* 254–347 K for **1b**, 274–325 K for **2b**; *d–r* 328–356 K for **1b**, 318–367 K for **2b**). The Arrhenius (Supporting Information, Figure S6) and Eyring plots were satisfactorily linear, and allowed the evaluation of the activation parameters reported in Table 3.

Table 3. Apparent activation parameters for the dynamic processes involving ion pairs **1b** and **2b**.

		$\Delta H^{\neq}$ [kJ mol^{-1}]	$\Delta S^{\neq}$ [J K^{-1} mol^{-1}]
1b	*ips*	66(1)	−3(2)
	d–r	80(2)	8(7)
2b	*ips*	57(1)	−23(4)
	d–r	75(1)	−7(4)

The kinetic parameters estimated for **2b** correspond to $\Delta G^{\neq}$ values of 15.3 kcal mol^{-1} for the *ips* and 18.4 kcal mol^{-1} for the *d–r* processes, at 300 K, in fair agreement with the values of 15.8(2) and 18.1(2) kcal mol^{-1}, reported in a previous investigation for the same ion pair.[8]

However, the above-reported values of the activation parameters (in particular the activation entropy close to zero) are not consistent with the dissociative nature inherent to the *ips* and the *d–r* mechanisms. Indeed, as discussed in the following paragraph, intermolecular processes can contribute to the observed exchange rate. Therefore the activation parameters of Table 3 must be considered apparent, and do not correspond to the true activation parameters for the *ips* or *d–r* processes.

Intermolecular exchanges emulating *ips* or *d–r* processes: We have got clear evidence that intermolecular $[MeB(C_6F_5)_3]^-$ or $B(C_6F_5)_3$ exchange processes can occur, that mimic the effects of the above described *ips* or *d–r* mechanisms.

It has already been observed[6] that the addition of $Li^+[MeB(C_6F_5)_3]^-$ (acting as a source of "free" $[MeB(C_6F_5)_3]^-$ anion) to C_6D_6 solutions of *ansa*-zirconocene contact ion pairs significantly increased the rate of indenyl symmetrization by associative attack of $[MeB(C_6F_5)_3]^-$ to the Zr center.[31]

We have now found that the presence of "free" $[MeB(C_6F_5)_3]^-$ anion has an analogous effect in the case of our bisindenyl ion pairs. This has been ascertained by examining samples obtained by treating [D_8]toluene solutions of **1a** with an amount of $B(C_6F_5)_3$ smaller than one equivalent. In these conditions, mixtures of **1b** and of the dinuclear methyl bridged ion pair $[\{(4,7\text{-}Me_2indenyl)_2ZrMe\}_2(\mu\text{-}Me)]^+[MeB(C_6F_5)_3]^-$ (**3**, Figure 7) were formed (Figure S7).

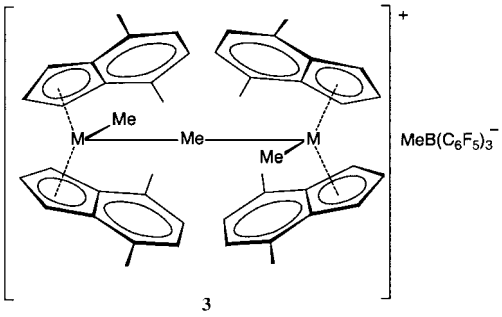

3

Figure 7.

Similar dinuclear species have been previously reported for related zirconocene complexes,[5,32,33] and it was pointed out that they (at least in sufficiently diluted solutions)[5] exist as solvent-separated ion pairs, rather than as contact ion pairs.[34] In the room temperature ^{1}H NMR spectra of the above mixtures containing **1b** and **3**, all the signals of **1b** (but that of Me–Zr) were broadened with respect to what observed in the same conditions in the absence of **3** (Figure 8). The fact that the Me–Zr resonance of **1b** remained sharp indicates that the broadening of the other resonances cannot arise from any exchange process involving the whole **1b** ion pair, nor from the exchange between the zirconocene units of **1b** and **3** (which does exist, but has a much longer time scale).[35] The observed broadening therefore must arise from an intermolecular contribution to the anion exchange process: indeed 2D EXSY maps (above 233 K) showed exchange between the $[MeB(C_6F_5)_3]^-$ anion of ion pair **1b** and that of **3**. Addition of $B(C_6F_5)_3$ to the above mixtures destroyed the dimeric species **3**, according to Reaction (2), and caused the sharpening of all the previously broadened resonances (Figure 8), including that of Me–B (better observed in ^{11}B-decoupled spectra). The last observation confirms that the increase of the rate of indenyl symmetrization in the presence of **3** is due to an intermolecular exchange involving the $[MeB(C_6F_5)_3]^-$ anion (the simple exchange of the anion position according to the *ips* mechanism obviously would not cause any broadening of the Me-B signal).

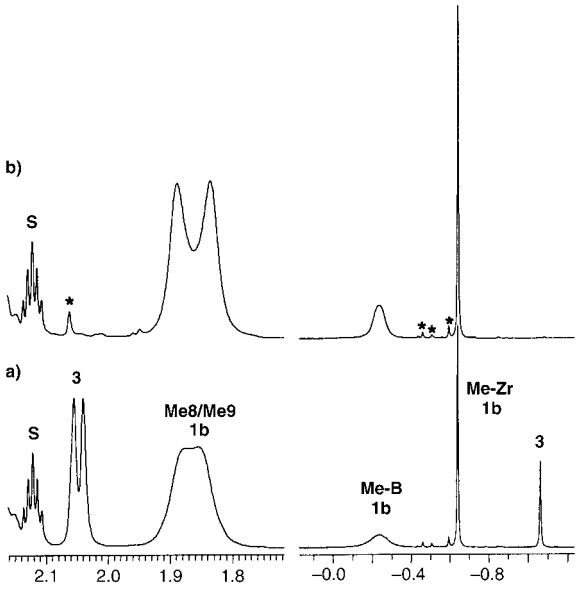

Figure 8. Selected regions of ^{1}H NMR spectra of **1b** at 300 K: a) in the presence of the dimeric species **3** (58 mM); b) after destruction of **3**, by further $B(C_6F_5)_3$ addition (66 mM). The asterisks mark some impurities, while S indicates the toluene signal.

$$[\{(4,7\text{-}Me_2\text{indenyl})_2ZrMe\}_2(\mu\text{-}Me)]^+\,[MeB(C_6F_5)_3]^- + B(C_6F_5)_3 \rightarrow 2\,[(4,7\text{-}Me_2\text{indenyl})_2ZrMe]^+\,[MeB(C_6F_5)_3]^- \quad (2)$$

Intermolecular exchange processes played a role even in samples generated in situ from "exact" zirconocene/$B(C_6F_5)_3$ stoichiometry (as judged by the absence of spectroscopically detectable amounts both of the dimeric species **3** and of free borane). Indeed dilution experiments on **1b** samples at 300 K showed a progressive sharpening of the resonances of the indenyl protons and of Me–B (the latter effect better detected in ^{1}H{^{11}B} spectra). The kinetic constants for indenyl symmetrization (evaluated from the bandwidth of Me8 and Me9 signals) decreased linearly with the concentration, in the range from 40 to 6 mM, with non-zero intercept (Figure 9). This indicates that both monomolecular and bimolecular processes contribute to the observed exchange rate.

The monomolecular process should correspond to the true *ips* mechanism and its rate at 300 K has been estimated from the intercept of the straight lines fitting the k_{obs}/concentration data ($k = 12.1(1)\ s^{-1}$, notably constant in different dilution experiments, even though k_{obs} values lie on lines with different slopes, see Experimental Section).

The bimolecular mechanism might involve the aggregation of two **1b** ion pairs in a transition state which should resemble the ion quadruples described by Brintzinger et al.[6,36] However, this would not explain the observed variation of the bandwidth of the Me–B signal, which can arise only from the presence of an exchange partner, that is, a different ion pair containing a $[MeB(C_6F_5)_3]^-$ anion. Such partner has been detected by 2D EXSY experiments at 300 K

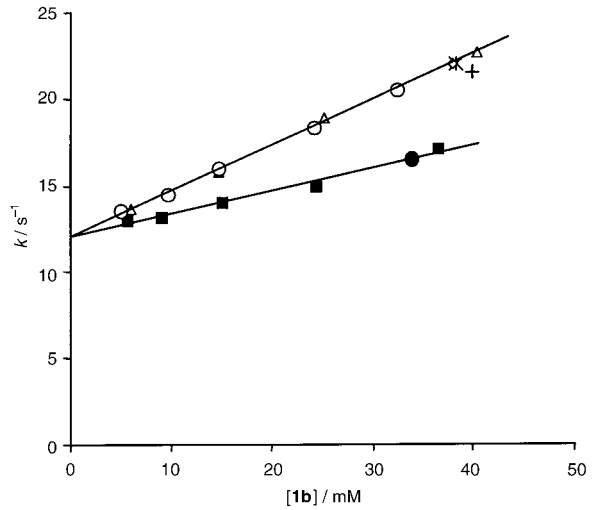

Figure 9. Plot of the rate constants for indenyl symmetrization in **1b** (evaluated from the Me8–Me9 bandwidths) vs **1b** concentration (300 K). The symbols △, ○ and ■ indicate data from three dilution experiments, while the other points (◇, +, *, and ●) refer to different samples.

(Figure S9, Supporting Information), that showed an exchange crosspeak between Me–B of **1b** and a very weak and broad resonance, undetectable in the normal 1D spectrum; the δ value shifted from 0.84 to $\approx$1.10 ppm on decreasing the concentration. This resonance can be attributed to a loosely bound $[MeB(C_6F_5)_3]^-$ anion,[37] in some unidentified ion pair,[38,39] We think that such ion pair was a by-product, rather than an inherent constituent of the zirconocene/$B(C_6F_5)_3$ system, because of some variability of the kinetic constants for indenyl symmetrization evaluated in different experiments at comparable concentration (see Figure 9).

The variation of the bandwidth of the Me–B signal of **1b**, in ^{1}H{^{11}B} spectra at different concentrations (Figure 10a), allowed the estimate of the rate constants for this intermolecular anion exchange. The constants well corresponded to twice the intermolecular contribution to indenyl symmetrization (Figure 10b), in line with an associative symmetric transition state, containing two equivalent $[MeB(C_6F_5)_3]^-$ anions.[40]

The observed anion exchange rates result therefore from two contributions: the true *ips* mechanism and the intermolecular exchange with loosely bound $[MeB(C_6F_5)_3]^-$ anions of other ion pairs (such as the dimeric species **3** or some unidentified impurity).

An analogous behavior was observed for **2b**: the rate of exchange of the $[MeB(C_6F_5)_3]^-$ site was affected by the dilution (Figure S10, Supporting Information) and by the presence of the "free" $[MeB(C_6F_5)_3]^-$ anion (as counterion of the dimeric cation formed in situ by treating **2a** with less than one equivalent of borane).

As expected, the presence of an excess of $B(C_6F_5)_3$, with respect to the 1:1 stoichiometry, did not affect the rate of exchange of the $[MeB(C_6F_5)_3]^-$ anion (i.e., the *ips* process), both for **1b** and **2b**.

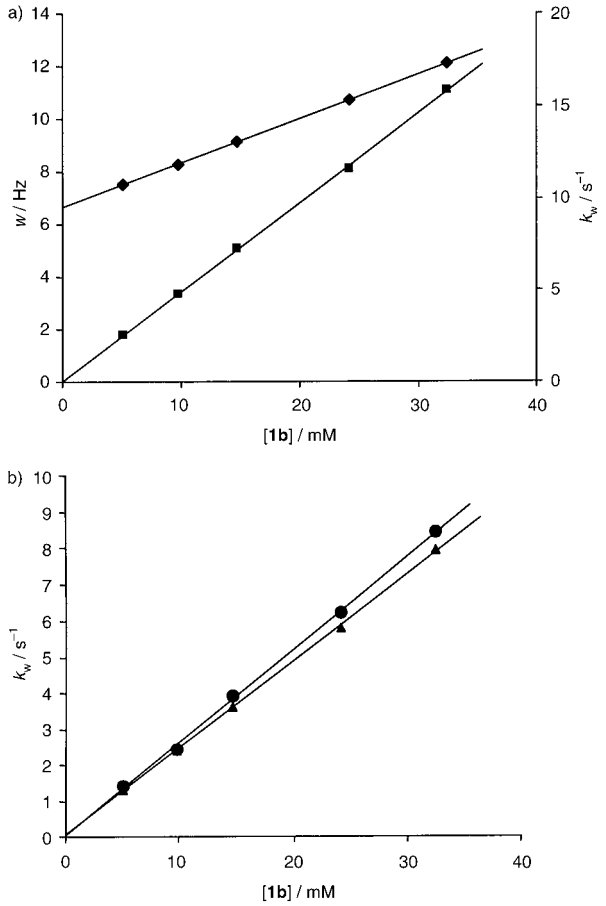

Figure 10. a) Plot of the bandwidth w of the Me–B signal of **1b**, measured in $^1H\{^{11}B\}$ spectra, at different concentrations, at 300 K (◆), and of the corresponding k_w (■), evaluated as $k_w=\pi(w-w^0)$, where w^0 is the intercept of the w/[**1b**] plot; b) comparison of $k_w/2$ (▲) to the intermolecular contribution to indenyl symmetrization (●), obtained by subtracting k_{ips} (the intercept of Figure 7, 12.1 s^{-1}) to the kinetic constants for indenyl symmetrization evaluated in the same experiment (represented by ○ in Figure 7).

As to the *d–r* mechanism, dilution experiments performed at 347 K on [D_8]toluene solutions of both ion pairs **1b** and **2b**, generated in situ by using exactly one equivalent of $B(C_6F_5)_3$, did not cause any significant variation of the bandwidth of the Me–Zr signal. Therefore in these conditions intermolecular processes do not contribute significantly to the exchange of $B(C_6F_5)_3$ between the two methyl groups.

However, the rate of the latter process was increased by the presence of $B(C_6F_5)_3$ in excess. This has been unambiguously ascertained by a series of 2D ^1H EXSY measurements, performed at 320 K on a [D_8]toluene solution of **1b** treated with increasing amounts of $B(C_6F_5)_3$: the kinetic constants describing the Me-Zr/Me-B exchange (k_{obs}) increased linearly with $B(C_6F_5)_3$ concentration (Figure 11), according to a classical $k_{obs}=k_1 + k_2[B(C_6F_5)_3]$ relationship, with $k_1=1.5(2)$ s^{-1} and $k_2=52(3)$ s^{-1} M^{-1}.

The accelerating effect of free $B(C_6F_5)_3$ can be explained by assuming that the Lewis acid is able to attack the Me–Zr group of the adduct **1b**, resulting in the formation of an ion pair in which two $[MeB(C_6F_5)_3]^-$ anions strongly interact

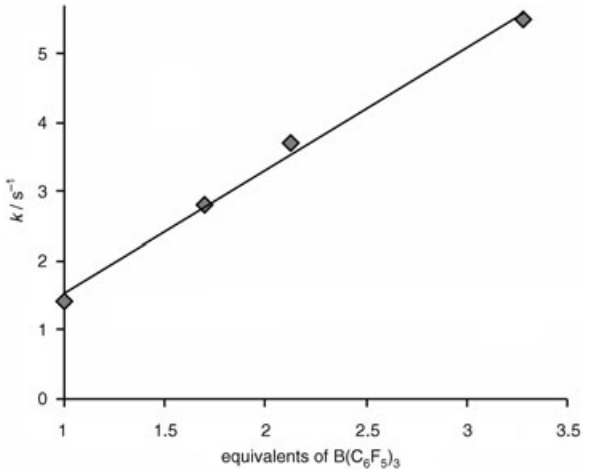

Figure 11. Plot of the rate constants concerning borane exchange in **1b** vs equivalents of $B(C_6F_5)_3$, measured at 320 K.

with the $[(indenyl)_2Zr]^{2+}$ cation.[41] The lifetime of this high energy species (possibly just a transition state) is expected to be short and its rate determining formation should be followed by fast elimination of one of the $B(C_6F_5)_3$ molecules, leading eventually to a result analogous to that of the *d–r* exchange.

Conclusion

Two main results have been provided by the present investigation. From the point of view of the solution structure of the species arising from the interaction of $B(C_6F_5)_3$ with zirconocenes **1a** and **2a** of Figure 2, it has been confirmed that at low temperature they are present as contact ion pairs, in which the $[MeB(C_6F_5)_3]^-$ anion occupies a specific position in the coordination sphere of the $[(indenyl)_2ZrMe]^+$ cation. The observation of selected NOE correlations between the methyl ligands and some indenyl protons demonstrated that in solution a few preferred rotamers are present; their enantiomerization, fast even at the lowest temperatures, creates the apparent C_s symmetry that equalizes the two indenyl moieties. Most significantly, it has been shown that molecular mechanics computations, guided by the experimentally observed NOE correlations, can provide reliable information on the solution conformers even for a system with a flat potential energy surface, such as that constituted by a zirconocene with relatively unhindered cyclopentadienyl-like substituents. To the best of our knowledge, this is the first time that such analysis has been applied to a zirconocene ion pair without *ansa*-bridge or bulky substituents; however, a similar approach has been previously reported for other types of zirconium complexes.[19]

From the point of view of the dynamics, both the exchange processes previously described[6–8] for this type of ion pairs have been observed, the exchange of the coordination sites between the methyl and the $[MeB(C_6F_5)_3]^-$ anions (the *ips* process) being much faster (about three orders of magnitude) than $B(C_6F_5)_3$ transfer between the two methyl groups

(the *d–r* process). This is in line with previous findings concerning ion pairs involving the strong Lewis acid $B(C_6F_5)_3$.[7] However, we have also shown that when the ion pairs are generated in situ, by $B(C_6F_5)_3$ addition to the zirconocene complexes, intermolecular exchange processes may occur, that can mimic the effects of the *ips* or *d–r* mechanisms. Our data suggest that such intermolecular processes are not inherent to the zirconocene–$B(C_6F_5)_3$ system, but rather arise from inexact stoichiometry or adventitious impurities. Therefore the contradiction between the Marks and Brintzinger reports might arise mainly from differences in the experimental methodologies: in the Marks work the ion pairs are isolated and purified, while in the Brintzinger work the ion pair are generated in situ, as in the present investigation.

The accelerating effect of $B(C_6F_5)_3$ excess on the Me–B/Me–Zr exchange is of interest, since it implies the formation, at least as a transition state, of a dicationic bis-methylborate adduct. Such kinetic effect was previously observed in some *ansa*-zirconocenes ion pairs,[6] whilst for a number of non-*ansa* biscyclopentadnienyl dimethyl metal complexes[3,42] it had been shown that an excess of $B(C_6F_5)_3$ not only does not effect the removal of the second methyl group (as in the present case),[41] but also does not affect the rate of the *d–r* process. Most likely, $B(C_6F_5)_3$ attack on the Zr–Me site of the ion pair is affected not only by the steric hindrance,[43] but also by electronic factors: in particular, the electrophilic attack on the $[(indenyl)_2ZrMe]^+$ cations might be a consequence of the softer nature of these species with respect to $[(cyclopentadienyl)_2ZrMe]^+$, due to the higher donor power of the indenyl groups.

Experimental Section

General procedures: All the manipulations were performed under nitrogen using oven dried Schlenk-type glassware. $B(C_6F_5)_3$ (Boulder Scientific) was purified by continuos extractions with refluxing *n*-pentane (final water content ca. 0.15% *w/w*, as determined by Karl-Fischer analysis). All the experiments have been performed in deuterated toluene (C.I.L., Isotec Inc. or Sigma-Aldrich) dried on activated molecular sieves 4 Å). The NMR spectra were acquired on a Bruker AVANCE DRX-300, AMX-500 or AC-200 spectrometers. The figures in the paper and in the Supporting Information generally show experiments performed at 7.1 T except when otherwise specified. ^{19}F NMR spectra were referenced to external $CFCl_3$ ($\delta = 0$ ppm) and ^{11}B NMR spectra to external $Et_2O{\cdot}BF_3$ ($\delta =$ 0 ppm). The temperature was calibrated with a standard CH_3OH/CD_3OD solution for the range 188–300 K, and with a standard ethylene glycol/[D_6]DMSO solution for the range 300–350 K.

The samples of the $[(indenyl)_2ZrMe]^+[MeB(C_6F_5)_3]^-$ ion pairs were prepared in situ, according to the following typical procedure: equimolar amounts of $B(C_6F_5)_3$ and zirconocene (ca. 20 mg) were separately weighted under N_2 in two NMR tubes and dissolved in weighted amounts of dried [D_8]toluene; then the solution of $B(C_6F_5)_3$ was added to that of the zirconocene.

For quantitative analysis of the cross peak volumes of the 2D EXSY/NOESY experiments, the employed relaxation delays were about three times the longest T_1.

In order to obtain the values of the rate constants for the various fluxional processes by band-shape analysis, when necessary all the scalar coupling constants for the observed nuclei have been determined (using the software WINDAISY), before the simulation of dynamic NMR spectra (using the software WINDYNAMICS). The chemical shifts at high temperature were established through the temperature dependence of the δ values measured in a temperature range where the system was static on the NMR time scale.

NMR data for $[(4,7\text{-}Me_2indenyl)_2ZrMe]^+[MeB(C_6F_5)_3]^-$ (1b): The ^1H NMR assignments (Table 1) have been performed through the 2D ^1H NOESY experiment shown in Figure 3 (211 K, $\tau_m = 0.2$ s). The following δ data at 298 K have taken into account the observed temperature dependence of the chemical shifts: δ = 6.6–6.4 (br m, H5 and H6), 5.76 (br, H3), 5.73 (pseudo t, H2), 5.67 (br, H1), 1.89 (br s, Me8), 1.84 (br s, Me9), −0.24 (br, Me-B), −0.64 (s, Me-Zr), $^3J(H1,H2) = 3.6$, $^4J(H1,H3) = 2.45$, $^3J(H2,H3) = 3.46$, $^3J(H5,H6) = 7.16$ Hz; the ^{13}C NMR signals (Figure S5a) have been assigned through standard 2D $^1H/^{13}C$ HMQC (203 K) and HMBC (298 K) experiments): δ = 103.0 (C1), 115.3 (C2), 102.8 (C3), 132.1 (C4), 127.4 (C5), 127.4 (C6), 132.9 (C7), 18.2 (C8), 18.4 (C9), 127.3 (C3a), 126.9 (C7a), 47.1 (Me–Zr), ≈20 (Me–B) (buried under the CD_3 septuplet of [D_8]toluene). The identification of the quaternary carbon atoms comes from the previous observation that in aromatic systems $^3J(C,H) > {}^2J(C,H)$.[44] At room temperature the signals of C1 and C3 coalesced, as well as those of Me8 and Me9, while the signals of C5 and C6 are hidden by the aromatic protons of the solvent (Figure S5); ^{19}F NMR (300 K): δ = −132.9 (m, *ortho*), −159.4 (t, *para*) and −164.4 (m, *meta*); ^{11}B NMR (300 K): δ = −13.7 ($\Delta\nu_{1/2} = 22$ Hz).

Dynamic behaviour of 1b: The kinetic constants for the *ips* mechanism have been obtained by: i) ^1H band shape analysis of the AB spin system due to H5 and H6 and of the singlets due to Me8 and Me9 in the temperature range 284–347 K and ii) volume analysis of Me8/Me9 exchange cross peaks in 2D ^1H NOESY/EXSY spectra (254 and 274 K). The rate constants for the *d–r* mechanism have been obtained from the bandwidth of the Me-Zr signal in high temperature ^1H spectra (328–356 K), and by the exchange cross peak between Me–Zr and Me–B in a 2D ^1H NOESY/EXSY at 300 K.

Dilution experiments on 1b: Three different samples of **1b** (ca. 40 mM) were prepared, directly into the NMR tube, as above described. Their ^1H NMR spectra were acquired and then the samples were progressively diluted. In order to maintain constant the volume of the solution in the NMR tube (to avoid changes of the bandwidth of the signals due to changes in instrumental homogeneity), portions of the solutions in the NMR tube were removed before addition of a corresponding amount of fresh toluene (the amounts of removed solutions and those of added solvent were measured by weighting). The kinetic constants for indenyl symmetrization were evaluated by band-shape analysis of the Me8–Me9 resonances. Figure 9 shows the three data series, whose fitting gave the following straight lines: (■) $k = 12.08(17) + 0.130(8)$ [**1b**], (○) $k = 12.12(10) + 0.257(5)$ [**1b**], (△) $k = 12.03(9) + 0.263(4)$ [**1b**]. In Figure 9 we have reported also other kinetic constants (marked with ◇, +, ●, and *), evaluated in spectra acquired during other experiments, different from the dilution series here described: also, in these cases most of the data lie on (or close to) the steeper lines, but one. The experiments, including the dilution series, were performed by using reactants arising from different preparations or purification procedures: however, no correlation was found between the experimental data and the reactant origins, nor with any other reaction condition or detectable impurity. In particular, we checked that the presence of an excess of $B(C_6F_5)_3$, up to 1 equiv, did not cause any significant change of Me8 and Me9indenyl bandwidths at 300 K. The kinetic constants for the intermolecular exchange of $[MeB(C_6F_5)_3]^-$ anion were evaluated from the linewidth of the Me–B signal in $^1H\{^{11}B\}$ spectra, since the signal of the exchanging partner at ≈1 ppm was too weak and broad to allow any reliable evaluation of the kinetic constants from the 2D maps.

Influence of $B(C_6F_5)_3$ concentration on the rate of the Me–B/Me–Zr exchange in 1b: A 34 mM solution of **1b** in [D_8]toluene was prepared directly in the NMR tube, as above described, and a 2D ^1H EXSY was recorded at 320 K ($\tau_m = 0.3$ s). The absence of free $B(C_6F_5)_3$ was checked, then three different amounts of $B(C_6F_5)_3$ were added in the NMR tube and 2D ^1H EXSY spectra were recorded after each addition, at the same temperature. From the volume of the Me–B/Me–Zr crosspeak, the fol-

lowing rate constants were computed: k /s^{-1} (in parenthesis the concentration of free $B(C_6F_5)_3$ /mM), 1.4 (0), 2.8 (24), 3.7 (38), 5.5 (78) (see Figure 11). $B(C_6F_5)_3$ additions caused also a slight but measurable increase of Me–Zr linewidth: 1.90, 1.99, 2.22, and 2.95 Hz.

NMR data of $[(indenyl)_2Zr(Me)]^+[MeB(C_6F_5)_3]^-$ (2b): The ^{1}H NMR assignments have been performed through a 2D ^{1}H COSY experiment (248 K, 4.7 T); the results are shown in Figure S1 of Supporting Information: 248 K: δ = 6.84 (m, H7), 6.78 (m, H4), 6.69 (m, H5), 6.60 (m, H6), 5.68 (m, H3), 5.50 (pseudo t, H2), 5.18 (m, H1), −0.36 (br, Me-B), −0.48 (s, Me-Zr); following the variation with the temperature of the chemical shifts, resonances have been attributed also at 300 K (C_7D_8, 7.1 T): δ = 6.93 (m, H7), 6.83 (m, H4), 6.74 (m, H5 and H6), 5.74 (br m, H3), 5.61 (pseudo t, H2), 5.42 (br m, H1), −0.19 (br, Me-B), −0.54 (s, Me-Zr), ^3J(H1,H2) = 3.4, ^4J(H1,H3) = 2.1, ^5J(H1,H4) = 1.0, ^6J(H1,H5) = −0.15, ^3J(H2,H3) = 3.4, ^5J(H2,H4) = 0.1, ^3J(H4,H5) = 8.7, ^4J(H4,H6) = 1.3, ^5J(H4,H7) = −1.5, ^3J(H5,H6) = 6.7 Hz; ^{13}C NMR: the attributions have been obtained through 2D HMQC and HMBC ^{1}H/^{13}C experiments (300 K): δ = 148.6 (m, ^1J(C,F) = 234 Hz, CF *ortho* or *meta*), 137.6 (m, ^1J(C,F) = 244 Hz, CF *meta* or *ortho*), 139.5 (m, ^1J(C,F) = 250 Hz, CF *para*), 127.7 (C5, C6), 126.0 (C3a, C7a), 125.6 (C4), 125.4 (C7), 119.1 (C2), 103.4 (C3), 102.5 (C1), 47.9 (Me-Zr), ≈20 (Me-B, overlapped with the CD_3 multiplet of the deuterated solvent); ^{19}F NMR (300 K): δ = −133.1 (m, *ortho*), −159.4 (pseudo t, *para*), −164.4 (m, *meta*); ^{11}B NMR (300 K): δ = −13.9 ppm ($\Delta\nu_{1/2}$ = 23 Hz).

Dynamic behavior of 2b: A 2D ^{1}H EXSY experiment at 300 K showed a strong cross peak between the indenyl protons H1 and H3 (the signals of the four aromatic protons H4–H7 were too close to allow unambiguous detection of their crosspeaks), whilst the correlation between Me–B and Me–Zr (diagnostic of the *d–r* mechanism) was much weaker than the H1/H3 one. An analogous EXSY experiment at 253 K showed the H1/H3 correlation only (k = 0.72 s^{-1}), that was detectable even at a temperature as low as 234 K. The kinetic constants for the *ips* mechanism have been estimated by band shape analysis of the resonances of H1 and H3 in the temperature range 274–325 K, and those for the *d–r* process (318–367 K) have been obtained from band shape analysis of the Me–Zr signal, the broadening of which became detectable only at temperatures higher than 300 K. The effect of **2b** concentration on the rate of the *ips* process has been checked by a dilution experiment, performed as described for **1b** (Supporting Information, Figure S10).

$[\{(4,7\text{-}Me_2indenyl)_2ZrMe\}_2(\mu\text{-}Me)]^+[MeB(C_6F_5)_3]^-$ (3): The ^{1}H NMR resonances of **3** have been identified from a low temperature (233 K) 2D ^{1}H NOESY experiment performed on a sample containing both **1b** and **3** ([D_8]toluene, τ_m = 0.25 s). The two high-field signals at δ −2.40 and −1.13 ppm (ratio 1:2) are due to the bridging and terminal Zr-bound methyl groups, respectively. The ^{1}H NMR resonance of the $[MeB(C_6F_5)_3]^-$ anion (δ 1.54 at 233 K, 1.38 at 300 K) has been easily identified from its exchange cross peak with Me–B of **1b** (observed even at 233 K), and its δ is in full agreement with literature data.[5] The indenyl resonances of **3** have been identified from their NOE crosspeaks with the two Zr-bound methyl groups; their attributions followed straightforwardly, based, as usual, on arbitrarily labelling as H1 the highest field signal of the H1/H3 couple (at 233 K the signals of Me8 and Me9, as well as those of H5 and H6 are accidentally overlapped): δ (233 K) = 2.04 (pseudo s, Me8 and Me9), 5.67 (m, H1), 5.80 (m, H2), 5.89 (m, H3), 6.66 (pseudo s, H5 and H6); ^{13}C NMR (300 K): δ = 148.6 (m, ^1J(C,F) = 243 Hz, CF *ortho* or *meta*), 137.6 (m, ^1J(C,F) = 251 Hz, CF *meta* or *ortho*), 139.5 (m, ^1J(C,F) = 249 Hz, CF *para*), 101.30 (C1), 114.22 (C2), 102.29 (C3), 126.45 (C5/C6), 126.71 (C6/C5), 18.57 (C8/C9), 19.04 (C9/C8), 44.53 (Me-Zr), 21.39 (μ-Me). The signals of Me-B and of the quaternary carbons have not been identified. ^{19}F NMR (300 K): δ = −131.8 (*ortho*), −164.4 (*para*), −166.6 (*meta*).

NMR data of $[(indenyl)_2Hf(Me)]^+[MeB(C_6F_5)_3]^-$: ^{1}H NMR (278 K, 4.7 T): δ = 6.86 (m, H7), 6.81 (m, H4), 6.71 (m, H5), 6.61 (m, H6), 5.50 (pseudo t, H2), 5.46 (m, H3), 5.20 (m, H1), −0.016 (br, Me-B), −0.71 (s, Me-Zr); ^{13}C NMR (300 K): δ = 148.6 (^1J(C,F) = 238, CF *ortho* or *meta*), 137.6 (^1J(C,F) = 249, CF *meta* or *ortho*), 139.5 (^1J(C,F) = 256, CF *para*), 127.7 (C5 and C6), 125.6 (C4), 125.2 (C7), 119.0 (C2), 101.4 (C3), 100.3 (C1), 45.4 (Me-Zr), 18.1 (Me-B).

Computational study: All the molecular mechanics computations have been performed with TINKER,[45] employing the MM3 functional form.[46] The description of the bisindenyldimethylzirconium moiety has been taken from the force field developed by Erker and co-workers.[47] Some new atom types have been introduced to describe the carbon atoms of the indenyl moiety and the methyl group bridging the boron and the zirconium atoms. The force field has been parameterized in order to reproduce the molecular geometry of a set of seven ion pairs;[48] the coordinates have been obtained from the Cambridge Crystallographic Data Centre.[25] Some of the force constants have been estimated by HF/3-21G(*) computations[51] on $[MeB(C_6F_5)_3]^-$ and $[Cp_2ZrMe]^+[MeB(C_6F_5)_3]^-$. At the and of the parameterization process, the mean absolute errors on a set of 56 bond distances, 91 bond angles, and 77 torsional angles were 0.009 Å, 1.63°, and 6.3°, respectively. A more detailed description of the force field accuracy with respect to different type of geometrical parameters, together with a complete description of the force field employed, can be found in the Supporting Information.

Effective distances $d_{ij,effective}$ employed in the interpolation of the observed NOE intensities have been computed in two steps. First of all, the methyl groups rotation, assumed to be faster then the overall tumbling, has been taken into account following the Tropp's equation:[52]

$$r_{Tropp} = \left(\frac{1}{2N} \sum_{\mu=1}^{N} \sum_{\nu=1}^{N} \frac{3(\mathbf{r}_\mu \cdot \mathbf{r}_\nu) - r_\mu^2 r_\nu^2}{r_\mu^5 r_\nu^5} \right)^{-1/6}$$

in which N is the number of interproton vectors $\mathbf{r}$ to be averaged (N = 3 for the interaction of a single proton with a methyl group, and N = 9 for the interaction between two methyl groups).

Subsequently, distances involving normal and primed atoms (see Figures 5 and 6) have to be averaged due to the enantiomerization process that leads to an apparent C_s symmetry of the ion pair. This process, requiring the rotation of the indenyl groups around the Zr–cp axis and the inversion of the chiral conformation of the $B(C_6F_5)_3$ moiety, is expected to be slower than the overall molecular correlation time, therefore the r^{-6} averaging limit equation applies:[53]

$$d_{effective} = \left(\frac{1}{M} \sum_{\lambda=1}^{M} r_\lambda^{-6} \right)^{-1/6}$$

in which M is the number of distances to be averaged; M = 2 for interactions involving Me–Zr or Me–B, for instance r(Me-Zr···H1) and r(Me-Zr···H1′); M = 4 for interactions involving the indenyl resonances only, for instance r(H1···H3), r(H1···H3′), r(H1′···H3), and r(H1′···H3′).[54]

Acknowledgement

The authors are grateful to Dr. Luigi Resconi for many helpful discussions and suggestions, and for providing the metallocene samples. T.B. and G.D. acknowledge Basell Polyolefins for partial funding of this work. Thanks are also due to the Italian CNR (ISTM) for providing facilities for low-temperature and inert atmosphere manipulations. Finally, the authors thank an anonymous referee for the careful, detailed and stimulating observations.

[1] E. Y.-X. Chen, T. J. Marks, *Chem. Rev.* **2000**, *100*, 1391–1434.
[2] a) A. G. Massey, A. J. Park, *J. Organomet. Chem.* **1964**, *2*, 245–250; b) A. G. Massey, A. J. Park, *J. Organomet. Chem.* **1966**, *5*, 218–225.
[3] a) X. Yang, C. L. Stern, T. J. Marks, *J. Am. Chem. Soc.* **1991**, *113*, 3623–3625; b) X. Yang, C. L. Stern, T. J. Marks, *J. Am. Chem. Soc.* **1994**, *116*, 10015–10031.
[4] M. Bochmann, S. J. Lancaster, M. B. Hursthouse, K. M. A. Malik, *Organometallics* **1994**, *13*, 2235–2243.
[5] S. Beck, M.-H. Prosenc, H.-H. Brintzinger, R. Goretzki, N. Herfert, G. Fink, *J. Mol. Catal. A Chem.* **1996**, *111*, 67–79.

[6] S. Beck, S. Lieber, F. Schaper, A. Geyer, H.-H. Brintzinger, *J. Am. Chem. Soc.* **2001**, *123*, 1483–1489.
[7] a) P. A. Deck, T. J. Marks, *J. Am. Chem. Soc.* **1995**, *117*, 6128–6129; b) P. A. Deck, C. L. Beswick, T. J. Marks, *J. Am. Chem. Soc.* **1998**, *120*, 1772–1784.
[8] A. R. Siedle, R. A. Newmark, *J. Organomet. Chem.* **1995**, *497*, 119–125.
[9] a) C. Zuccaccia, N. G. Stahl, A. Macchioni, M.-C. Chen, J. A. Roberts, T. J. Marks, *J. Am. Chem. Soc.* **2004**, *126*, 1448–1464; b) N. G. Stahl, C. Zuccaccia, T. R. Jensen, T. J. Marks, *J. Am. Chem. Soc.* **2003**, *125*, 5256–5257.
[10] D. Balboni, I. Camurati, G. Prini, L. Resconi, S. Galli, P. Mercandelli, A. Sironi, *Inorg. Chem.* **2001**, *40*, 6588–6597.
[11] J. L. Atwood, W. E. Hunter, D. C. Hrncir, E. Samuel, H. Alt, M. D. Rausch, *Inorg. Chem.* **1975**, *14*, 1757–1762.
[12] Only in the presence of bulky substituents on the indenyl rings the dynamic process could be frozen on the NMR time scale. See for instance refs. [13]–[16].
[13] a) G. Erker, M. Aulbach, M. Knickmeier, D. Wingbermühle, C. Krüger, M. Nolte, S. Werner, *J. Am. Chem. Soc.* **1993**, *115*, 4590–4601; b) M. Knickmeier, G. Erker, T. Fox, *J. Am. Chem. Soc.* **1996**, *118*, 9623–9630; c) S. Knuppel, J.-L. Fauré, G. Erker, G. Kehr, M. Nissinen, R. Fröhlich, *Organometallics* **2000**, *19*, 1262–1268.
[14] R. Leino, H. J. G. Luttikhedde, A. Lehtonen, R. Sillanpää, A. Penninkangas, J. Strandén, J. Mattinen, J. H. Näsman, *J. Organomet. Chem.* **1998**, *558*, 171–179.
[15] M. D. Bruce, G. W. Coates, E. Hauptman, R. M. Waymouth, J. W. Ziller, *J. Am. Chem. Soc.* **1997**, *119*, 11174–11182.
[16] N. Schneider, F. Schaper, K. Schmidt, R. Kirsten, A. Geyer, H.-H. Brintzinger, *Organometallics* **2000**, *19*, 3597–3604.
[17] The generalized broadening of the resonances observed on lowering the temperature is due to the loss of resolution for increased viscosity of the solution.
[18] Interestingly, we observed exactly the same pattern of cross peaks in the analogous Hf ion pair $[(indenyl)_2HfMe]^+[MeB(C_6F_5)_3]^-$ (see Supporting information, Figures S3 and S4), in line with the close structural similarity between Zr and Hf derivatives, previously observed in several related cases (see ref. [15]).
[19] Solution structures have been derived from the NOE data following an approach similar to the 2DCPA (two-dimensional conformer population analysis) proposed by Landis. For recent applications of 2DCPA see: a) C. P. Casey, S. L. Hallenbeck, J. M. Wright, C. R. Landis, *J. Am. Chem. Soc.* **1997**, *119*, 9680–9690; b) J. M. Wright, C. R. Landis, M. A. M. P. Ros, A. D. Horton, *Organometallics* **1998**, *17*, 5031–5040.
[20] D. Neuhaus, M. P. Williamson, *The Nuclear Overhauser Effect in Structural and Conformational Analysis*, 2nd ed., Wiley-VCH, New York, **2000**, pp. 167–178.
[21] A set of 28 NOE intensities has been employed, taking into account all the correlations between the indenylic protons and the Me–Zr and Me–B groups, and all the inter-ring interactions but the ones involving contiguous positions (such as H1/H2, H2/H3, H3/Me8 or H3/H4 and so on) for which the *intra*-ring contribute is strongly prevailing. A complete list is reported in Tables 1 and 2 for **1b** and **2b**, respectively.
[22] $r^2_{adj} = 1-\frac{(n-k)\sum_{\mu=1}^{n}(I_{ij,\mu}-\hat{I}_{ij,\mu})^2}{(n-1)\sum_{\mu=1}^{n}(I_{ij,\mu}-\langle I_{ij}\rangle)^2}$, in which I_{ij} and $\hat{I}_{ij}$ are the observed and the extimated NOE intensities, respectively, n is the number of observations, and k is the number of conformations.
[23] The null hypothesis $w_\lambda = 0$ has been tested by means of the statistic $t=\frac{w_\lambda}{s_{w_\lambda}} = \frac{w_\lambda\sqrt{(n-k)\sum_{\mu=1}^{n}[(d_{ij,\mu})_\lambda^{-6}-\langle(d_{ij})_\lambda^{-6}\rangle]^2}}{\sqrt{\sum_{\mu=1}^{n}(I_{ij,\mu}-\hat{I}_{ij,\mu})^2}}$ which follows a Student's t distribution with $n-k$ degrees of freedom.
[24] The preliminary interpolation process led to the following rotamers: ($\tau_1=-18$, $\tau_2=18°$) and ($\tau_1=-54$, $\tau_2=-72°$) for **1b**; ($\tau_1=-54$, $\tau_2=-90°$) and ($\tau_1=18$, $\tau_2=-126°$) for **2b**. The final interpolation process has been done starting from this values covering $\pm18°$ in step of 2°.
[25] CSD (version 5.24, November 2002). F. H. Allen, *Acta Crystallogr. Sect. B Struct. Sci.* **2002**, *58*, 380–388.
[26] Differences in the cross peaks' pattern of this two species, despite their similarity, can be explained observing that, due to the arbitrariness in defining H1/H3 in the NMR spectra, the indenylic ring results to be numbered in a anticlockwise direction for **1b** and in a clockwise direction for **2b**, as shown in Figures 4 and 5.
[27] a) G. Jany, M. Gustafsson, T. Repo, E. Aitola, J. A. Dobado, M. Klinga, M. Leskela, *J. Organomet. Chem.* **1998**, *553*, 173–178; b) H. Schunmann, O. Stenzel, S. Dechert, R. L. Halterman, *Organometallics* **2001**, *20*, 1983–1991; c) Y. J. Cho, S. C. Yoon, W. S. Seo, B. W. Woo, B. J. Bae, I. H. Suh, J. T. Park, *Bull. Korean Chem. Soc.* **1999**, *20*, 362–364; d) W. A. Herrmann, J. Rohrmann, E. Herdtweck, W. Spaleck, A. Winter, *Angew. Chem.* **1989**, *101*, 1536–1538; *Angew. Chem. Int. Ed. Engl.* **1989**, *28*, 1511–1512; e) M. J. Burk, S. L. Colletti, R. L. Halterman, *Organometallics* **1991**, *10*, 2998–3000.
[28] The ^{19}F NMR spectra consist of three resonances, in the ratio 2:1:2, from 190 K up to room temperature, indicating the dynamic equivalence of the three rings and of the two *ortho* and the two *meta* positions within each ring.
[29] The broadening of the Me–B signal observed in Figure 1 on increasing the temperature is mainly due to the scalar coupling with quadrupolar boron isotopes, partially removed at lower temperatures ("thermal decoupling") for the progressively faster relaxation rates of the quadrupolar nuclei. This was confirmed by $^1H\{^{11}B\}$ spectra. Anyway, at room temperature (or higher) the bandwidth of the signal was affected also by the intermolecular exchange processes discussed below.
[30] For a series of $[(1,2\text{-}Me_2Cp)MMe]^+[MeBAr(C_6F_5)_2]^-$ ion pairs, containing different Ar substituents on boron and M = Zr or Hf, the rate of the *ips* process was found much smaller than borane dissociation–recombination.[7b] Only in the case of the ion pair generated by the strong Lewis acid $B(C_6F_5)_3$, the methide ion was bound so strongly to boron to make ion pair separation faster than borane dissociation.
[31] In ref. [6] (as well as in the present work) the term "free" indicates an "outer-sphere" or "non-covalently bound" methylborate anion, the existence of truly free $[MeB(C_6F_5)_3]^-$ being unrealistic in a nonpolar solvent such as toluene.
[32] M. Bochmann, S. J. Lancaster, *Angew. Chem.* **1994**, *106*, 1715–1718; *Angew. Chem. Int. Ed. Engl.* **1994**, *33*, 1634–1637.
[33] a) Y.-X. Chen, C. L. Stern, S. Yang, T. J. Marks, *J. Am. Chem. Soc.* **1996**, *118*, 12451–12452; b) Y.-X. Chen, T. J. Marks, *Organometallics* **1997**, *16*, 3649–3657; c) Y.-X. Chen, M. V. Metz, C. L. Stern, T. J. Marks, *J. Am. Chem. Soc.* **1998**, *120*, 6287–6305.
[34] In our solutions the ^1H resonance of the "free" methylborate anion is observed at δ 1.35, at room temperature in toluene (δ 1.54 at 233 K), in good agreement with the literature values for other dimeric species (δ 1.3–1.4 in benzene at 30 °C).[5]
[35] Indeed, the 2D NOESY maps at room temperature showed exchange between the cationic parts (monomeric and dimeric, respectively) of ion pairs **1b** and **3**: in particular, Me–Zr of **1b** exhibited exchange crosspeaks with both bridging and terminal methyl groups of **3**. This indicates fast dissociation–recombination of the dimeric cation, that is, exchange of a zirconocene molecule **1a** between two monomeric cations. The volumes of the cross peaks, as well as the bandwidth of the resonances of the Me–Zr groups of **1b** and **3** indicated that the rate of these processes was much smaller than that of the exchange of the corresponding anions. As expected, upon addition of the free zirconocene complex **1a**, also the signals of the latter species were involved in the exchange (Figure S8).
[36] S. Beck, A. Geyer, H.-H. Brintzinger, *Chem. Commun.* **1999**, 2477–2478.

[37] The weak and broad ^{19}F NMR resonances of this anion (δ −131.9 *ortho*, −163.0 *para*, −166.0 *meta*) have been identified through their exchange cross peaks with the corresponding signals of the $[MeB(C_6F_5)_3]^-$ anion of **1b** in 2D ^{19}F EXSY experiments.

[38] It has been previously observed that the ^1H NMR δ value represents a sensitive probe for the identity of the Me–B species.[39] The low-field shift upon dilution might reflect the increase of the fraction of solvent-separated Me–B anion (its ^1H NMR signal is close to δ 1.3).[5]

[39] S. Beck, M.-H. Prosenc, H.-H. Brintzinger, *J. Mol. Catal. A Chem.* **1998**, *128*, 41–52.

[40] In principle, the crosspeak observed in the 2D experiment could merely result from the dissociative *ips* process itself, without any additional kinetic significance. In this case, however, the rate of the Me–B exchange should not be concentration dependent.

[41] Relatively stable dicationic species have been obtained from the reaction of some metallocene dimethyl complex with two equivalents of $Al(C_6F_5)_3$, whilst the use of an excess of $B(C_6F_5)_3$ did not allow to remove the second methyl group: E. Y.-X. Chen, W. J. Kruper, G. Roof, D. R. Wilson, *J. Am. Chem. Soc.* **2001**, *123*, 745–746.

[42] F. Guerin, D. W. Stephan, *Angew. Chem.* **2000**, *112*, 1354–1356; *Angew. Chem. Int. Ed.* **2000**, *39*, 1298–1300.

[43] In the case of the most congested *ansa*-zirconocene complexes of ref. [6], $B(C_6F_5)_3$ excess did not cause any increase of the rate of indenyl symmetrization.

[44] F. Piemontesi, I. Camurati, L. Resconi, D. Balboni, A. Sironi, M. Moret, R. Zeigler, N. Piccolrovazzi, *Organometallics* **1995**, *14*, 1256–1266.

[45] J. W. Ponder, TINKER, Software Tools for Molecular Design, http://dasher.wustl.edu/tinker/

[46] N. L. Allinger, Y. H. Yuh, J.-H. Lii, *J. Am. Chem. Soc.* **1989**, *111*, 8551–8566.

[47] a) U. Höweler, R. Mohr, M. Knickmeier, G. Erker, *Organometallics* **1994**, *13*, 2380–2390; b) T. Jödicke, F. Menges, G. Kehr, G. Erker, U. Höweler, R. Fröhlich, *Eur. J. Inorg. Chem.* **2001**, 2097–2106.

[48] CSD-refcodes: BACXUY,[5] LIYKAF,[49] QEZXAU,[6] SOBTIM10, YEKKII, YEKKOO,[3b] and XIDKIE.[50]

[49] I. A. Guzei, R. A. Stockland Jr., R. F. Jordan, *Acta Crystallogr. Sect. C Cryst. Struct. Commun.* **2000**, *56*, 635–636.

[50] Z. Lui, E. Somsook, C. R. Landis, *J. Am. Chem. Soc.* **2001**, *123*, 2915–2916.

[51] Gaussian 98 (revision A.11.3), M. J. Frisch, G. W. Trucks, H. B. Schlegel, G. E. Scuseria, M. A. Robb, J. R. Cheeseman, V. G. Zakrzewski, J. A. Montgomery, R. E. Stratmann, J. C. Burant, S. Dapprich, J. M. Millam, A. D. Daniels, K. N. Kudin, M. C. Strain, O. Farkas, J. Tomasi, V. Barone, M. Cossi, R. Cammi, B. Mennucci, C. Pomelli, C. Adamo, S. Clifford, J. Ochterski, G. A. Petersson, P. Y. Ayala, Q. Cui, K. Morokuma, D. K. Malick, A. D. Rabuck, K. Raghavachari, J. B. Foresman, J. Cioslowski, J. V. Ortiz, A. G. Baboul, B. B. Stefanov, G. Liu, A. Liashenko, P. Piskorz, I. Komaromi, R. Gomperts, R. L. Martin, D. J. Fox, T. Keith, M. A. Al-Laham, C. Y. Peng, A. Nanayakkara, C. Gonzalez, M. Challacombe, P. M. W. Gill, B. G. Johnson, W. Chen, M. W. Wong, J. L. Andres, M. Head-Gordon, E. S. Replogle, J. A. Pople, Gaussian, Inc., Pittsburgh, PA, **2002**.

[52] P. F. Yip, D. A. Case in *Computational Aspects of the Study of Biological Macromolecules by Nuclear Magnetic Resonance Spectroscopy* (Eds.: J. C. Hoch, F. M. Poulsen, C. Redfield), Plenum Press, New York, **1991**, pp. 317–330.

[53] C. M. Fletcher, D. N. M. Jones, R. Diamond, D. Neuhaus, *J. Biomol. NMR* **1996**, *8*, 292–310.

[54] R. R. Ernst, G. Bodenhausen, A. Wokaun in *Principles of Nuclear Magnetic Resonance in One and Two Dimensions*, Oxford Science Publications, Belfast, **1987**, Chapter 9.

Received: June 16, 2004
Published online: November 25, 2004

